European Polymer Journal 49 (2013) 2748–2758

Contents lists available at SciVerse ScienceDirect

European Polymer Journal

journal homepage: www.elsevier.com/locate/europolj

Effect of high molar mass species on linear viscoelastic properties of polyethylene melts

Jon Otegui, Javier Ramos, Juan F. Vega *, Javier Martínez-Salazar

BIOPHYM, Departamento de Física Macromolecular, Instituto de Estructura de la Materia-Consejo-Superior de Investigaciones Científicas (IEM-CSIC), C/Serrano 113 bis, 28006 Madrid, Spain

ARTICLE INFO

Article history:
Received 22 November 2012
Received in revised form 29 May 2013
Accepted 11 June 2013
Available online 22 June 2013

Keywords:
Linear polyethylene
Molecular weight distribution
High molecular weight tails
Melt linear viscoelasticity
Reptation

ABSTRACT

The molecular features and the linear viscoelastic melt properties of a series of polydisperse high density polyethylene are investigated. The main molecular characteristic of the materials studied is the presence of high molar mass species, which give rise to unusual values of the M_z/M_w ratio. This molecular particularity strongly affects to the linear viscoelastic melt properties as the Newtonian viscosity and the steady-state shear recoverable compliance. Both the third and the fourth moments of the molecular weight distribution affect to the values of these properties, which follow the trend expected by the reptation model. The evidences clearly prove the effect not only of the polydispersity index, but more interestingly of the shape of the molecular weight distribution on the dynamics of the systems. The behavior shown by the experimental samples studied in this work is interesting as the linear viscoelastic properties have become widely used, not only to test the molecular weight distribution dependence of the viscoelastic fingerprint and the processability, but also to assess the possible presence of long chain branching.

1. Introduction

The effect of the molecular weight distribution (MWD) on the viscoelastic response of linear polyethylene (PE) melts has been widely reported in the literature since the 1960s, but the results are certainly contradictory. Bueche [1] and Graessley [2] considered the existence of an averaged molecular weight of the distribution, M_t, located between the second and the third moments, M_w and M_z, respectively, that best represents the average to explain the dependence of the Newtonian viscosity, η_0, in linear polymers with polydispersity index higher than $M_w/M_n = 2$. Later, Saeda and co-workers [3] found the experimental support to these ideas in polydisperse samples. Locati and Gargani [4] empirically expressed M_t in terms of the polydispersity index using Saeda's experimental data. In the same direction, Malkin and co-workers [5] proposed an empirical modification of the average molecular weight for the dependence of the rheological properties, later validated for polydisperse polypropylene (PP) [6,7] and PE [7]. The equation of Malkin and co-workers [5], obtained for polydisperse polybutadiene (PB), nicely agrees with recent theoretical predictions [8,9], based in the determination of the linear viscoelastic response from the MWD trace using the double reptation approach. The approximate correlation found by Nobile and Cocchini takes the form [8]:

$$\eta_0 = 0.51 K M_w^{\alpha} \left(\frac{M_z}{M_w}\right)^{\beta} \quad (1)$$

with K the corresponding pre-exponential constant for monodisperse species at a given temperature, $\alpha = 3.4$ and $\beta = 0.8$. This expression resembles the correlation found by den Doelder, but in this case with $\beta = 0.7$ [9]. Other authors did not observe these MWD effects on η_0 for polydisperse PE samples with $M_z/M_w = 2.2 \pm 0.7$ [10]. A more recent work has revealed that the width of the MWD

* Corresponding author. Tel.: +34 915 616 800; fax: +34 915 615 413.
E-mail address: jf.vega@csic.es (J.F. Vega).

0014-3057/$ - see front matter © 2013 Elsevier Ltd. All rights reserved.
http://dx.doi.org/10.1016/j.eurpolymj.2013.06.015

strongly affects to both η_0 and steady-state shear recoverable compliance, J_e^0, in linear PE samples with values of M_z/M_w between 4.0 and 11.2 [11,12]. It is widely accepted that J_e^0 does not relate to M_w, but it is very sensitive to the measure of the MWD. Many relations (empirical and theoretical) have been proposed to correlate J_e^0 with MWD. The one suggested by Mieras and van Rijn [13] (Eq. (2)) with power law exponent of $\gamma = 3.7$, was successfully tested by Mills [14] in polydimethylsiloxane (PDMS), polystyrene (PS) and PE.

$$J_e^0 \propto \left(\frac{M_z}{M_w}\right)^{\gamma} \tag{2}$$

The blending laws of Bogue et al. [15] and Kurata et al. [16] established values for γ of 2.0 and 3.7, respectively. More recently, Nobile and Cocchini [8] have obtained a similar correlation based in the double reptation approach, but with an exponent of $\gamma = 5.5$. Other correlations were proposed by Ferry et al. [17] based in the Rouse model, and Agarwal [18] from empirical observations, in which higher moments of the MWD are involved:

$$J_e^0 \propto \left(\frac{M_{z+1}M_z}{M_w^2}\right) \tag{3}$$

$$J_e^0 \propto \left(\frac{M_{z+1}M_z}{M_wM_n}\right) \tag{4}$$

By the other hand, Ressia et al. [19] proposed an expression based on the blending laws of Montfort et al. [20] and Zang et al. [21] for mixtures of monodisperse systems, which included not integer moments of the MWD ($Q_a = \Sigma w_i M_i^a$, with "a" values between 3.4 and 4.4):

$$J_e^0 \propto \left(\frac{Q_a}{Q_1^a}\right) \tag{5}$$

Finally, den Doelder has recently established a relationship based also on the double reptation model [9]:

$$J_e^0 \propto \left(\frac{M_z}{M_w}\right)^2 \left(\frac{M_{z+1}}{M_z}\right)^4 \tag{6}$$

From all these expressions strong effects of the highest moments of the MWD on the melt elastic character of polymeric materials are expected, as a slight increase in the moment ratios can cause values of J_e^0 several orders of magnitude higher than the characteristic value of monodisperse species.

In previous works we have reported that tridentate bis(imino)pyridyl iron complexes, when combined with a co-catalyst, such as methylaluminoxane (MAO) and aluminum alkyls ($AlEt_3$ and $AliBu_3$), form very active catalytic systems that yields linear PE with very broad MWD [22–24]. We have investigated the performance of this type of catalyst from the simulation [25–27] and experimental points of view [28]. We have also reported the effect of the MWD on η_0 for these materials in a recent contribution [29], on the basis of the applicability of Eq. (1). We must point out here that the reported values of M_z/M_w in the experimental PE samples studied in this work are extremely high, between 20 and 30 (2–3 times higher than those reported until now in linear polydisperse PE), so the effect of the very high-M_w tail has to be especially noticeable. For this reason, we extend the study of the physical properties of these materials and report: (i) basic physical properties of the materials; (ii) the effect of the presence of high-M_w tails on the melt linear viscoelastic properties, and more specifically on J_e^0, and (iii) the modeling of the linear viscoelastic response within the reptation framework by using the experimental MWD together with simulated values of the entanglement features.

2. Experimental methods

The materials were kindly supplied by Centro Tecnológico Repsol-YPF (Spain). The samples labeled from PE1 to PE4 listed in Table 1 were obtained from a bis(imino)pyridyl iron catalysts [28]. The polymerizations were carried out in a Buchi reactor (except the PE1 sample in Table 1, obtained in autoclave reactor in equivalent conditions and a slightly higher concentration of catalyst). Isobutene solvent (1 dm^3) and the required amount of MAO co-catalyst were introduced into the reactor under inert nitrogen atmosphere. The total pressure was adjusted to 40 bars. Reactions were carried out at a temperature of 90 °C and kept constant throughout the polymerization. In the Buchi series hydrogen was introduced continuously in the polymerization reactor to control the molecular weight of the final products. The total concentration of hydrogen is adjusted to remain constant during polymerization and increased from 0 to 1 mol% in the subsequent polymerizations (from PE2 to PE4). Polymerizations were carried out along 1 h. Two samples obtained from a metallocene single-site catalyst (mPE) have been included in this study, for comparison purposes [30].

The samples were analyzed by ^{13}C nuclear magnetic resonance (^{13}C NMR) on a Bruker DRX500 spectrometer. The spectra were recorded at 100 °C on a Bruker DRX 500 spectrometer operating at 125 MHz. The samples were dissolved in hot 1,2,4-trichlorobenzene (TCB) and d6-benzene. ^{13}C NMR results corroborate the linear structure of all the materials studied in this work in agreement with previous results [28].

The MWD of the samples was determined by means of high-temperature size exclusion chromatography (SEC) analyzer Waters 150C, equipped with refractive index (RI) and viscometer (V) detectors. All measurements were conducted at a flow rate of 1 mL min^{-1} and at temperature

Table 1
Molecular features of the samples studied.

Samples	M_w (kg mol^{-1})	M_w/M_n	M_z (kg mol^{-1})	M_{z+1} (kg mol^{-1})
	sd = ±5%			
mPE1[a]	65.0	3.6	195.0	585.0
mPE2[a]	152.0	2.3	350.0	805.0
PE1	35.0	6.1	1000	4730
PE2	49.4	7.8	1340	5770
PE3	71.7	9.7	1400	5300
PE4	92.5	13.3	1730	5200

[a] Single-site metallocene samples [30].

of 145 °C using 1,2,4-trichlorobenzene (TCB) as solvent. To accurately calibrate the column we have obtained the hydrodynamic volume, which is the product of the molecular weight, M; and the intrinsic viscosity, $[\eta]$, and the retention volume using monodisperse polystyrene standards (universal calibration). The viscometer detector makes this possible because it directly measures $[\eta]$, which is inversely proportional to the molecular density of the polymer coil. The molecular weight of the fractions has been estimated from the intrinsic viscosity values together using the hydrodynamic volumes obtained from of the universal calibration. True molecular weights can be obtained in this way independently of the chemical and molecular structure of the polymers and the calibration standards [31]. The Mark–Houwink correlation of the samples studied has a power law exponent of $\alpha_v = 0.70$ [30], in good agreement with literature results for linear PE [32–37], providing further evidence of the linear structure of the samples. The molecular features obtained by the SEC/RI/V system are listed in Table 1. The result obtained for each of the samples has been averaged from 10 independent measurements. The standard deviation of the averaged values obtained for the molecular features is s.d. = ±5%.

The thermal properties (melting point, T_m, and crystalline content, X_c) of the polymers were obtained on a Perkin Elmer 7 series thermal analyzer by heating to 160 °C at a rate of 10 °C min^{-1} and cooling at the same rate to 20 °C. A second heating cycle at 10 °C min^{-1} was used for data analysis. The reported T_m is the peak value from the last heating. Crystallinity was calculated using a value of 288.4 J g^{-1} as the reference melting enthalpy for 100% crystalline PE. The measured properties are listed in Table 2.

Small-amplitude oscillatory viscoelastic measurements in the melt were carried out by means of a Bohlin CVO stress-controlled rheometer using a parallel disk (15 mm diameter) geometry, in the angular frequency range between 10^{-2} and 10^{2} rad s^{-1}. The measurements were performed well inside the linear viscoelastic region (shear strain lower than 0.1) previously located by the aid of amplitude sweeps. The following viscoelastic functions were measured as a function of the angular frequency, ω, at different temperatures (between the melting temperature and 190 °C): storage shear modulus, G', and loss shear modulus, G''. The data obtained at the different temperatures were shifted along the angular frequency axis to a reference temperature of $T_R = 160$ °C. Vertical shifts along the modulus axis were not necessary. The frequency shift, a_T, was expressed in terms of the flow activation energy, E_a, using the Arrhenius relationship [35]:

$$a_T = \exp\frac{E_a}{R}\left(\frac{1}{T} - \frac{1}{T_R}\right) \tag{7}$$

with R the universal gas constant and T the absolute temperature. The values of E_a are given in Table 2.

For determining η_0 and J_e^0, creep and creep-recovery experiments were performed at $T = 160$ °C. The rheological tests were carried out using 25 mm parallel-plate and/or cone-plate geometries. We have ensured that the measurements were conducted in the linear viscoelastic regime and that the steady-state was reached in the preceding creep and the recovery tests by applying different stresses, τ_0, and creep times, t_c. It was proven that the stresses applied were within the linear viscoelastic regime (between 0.78 and 12.5 Pa in the materials studied here). The time-dependent deformation $\gamma(t)$ was measured. The quotient of the deformation and the applied stress is the creep compliance, $J(t)$:

$$J(t) = J_0 + \Psi(t) + \frac{t}{\eta_0} \tag{8}$$

being J_0 the instantaneous elastic compliance, $\Psi(t)$ the creep function and t/η_0 is the irreversible contribution to the deformation. If t_c is sufficiently long, $\Psi(t)$ will reach a constant value and η_0 reads as follows:

$$\eta_0 = \lim_{t\to\infty}\frac{t}{J(t)} \tag{9}$$

After a defined t_c, the applied stress was set to zero ($\tau_0 = 0$ Pa) and the recoverable deformation, and then the recoverable compliance, J_r, was measured as a function of the recovery time, t_r. If the creep and recovery time are long enough and the experiment is performed in the linear range of deformation, J_e^0 is obtained as:

$$J_e^0 = \lim_{\substack{t_c\to\infty \\ t_r\to\infty}} J_r(t_c, t_r) \tag{10}$$

It was proven that the thermal stability of the materials was sufficient for all measuring times at the applied temperature. The values (averaged over at least 3 independent

Table 2
Physical properties of the samples studied: density (ρ), melting temperature (T_m), crystallinity (X_c), flow activation energy (E_a); Newtonian viscosity (η_0) and steady-state shear recoverable compliance (J_e^0).

Samples	ρ (g cm^{-3})[a]	T_m (°C)	X_c (%)	E_a (kJ mol^{-1})	η_0 (kPa s)[b]	η_0 (kPa s)[c]	J_e^0 10^3 (Pa^{-1})[c]
mPE1	n.d.	n.d.	n.d.	23.8	1.09	n.d.	n.d.
mPE2	0.9516	134.2	0.70	23.0	23.4	23.0	0.055
PE1	0.9737	130.8	87.0	27.1	0.985	1.03	55.0
PE2	0.9716	133.2	86.0	25.0	3.38	3.12	39.2
PE3	0.9687	133.6	81.0	26.7	13.4	12.5	13.1
PE4	0.9705	134.1	78.0	27.9	25.0	24.2	8.65

n.d. Means not determined.
[a] Density measured on a gradient column.
[b] Newtonian viscosity, η_0, measured at $T = 160$ °C from dynamic measurements [29].
[c] Newtonian viscosity, η_0, and steady-state shear recoverable compliance, J_e^0, measured at $T = 160$ °C from creep measurements.

measurements) obtained for both η_0 and J_e^0 are listed in Table 2. The standard deviation of the averaged values obtained for the molecular features is s.d. = ±6.5%.

3. Results and discussion

The ^{13}C NMR analysis reveals that all the products obtained from the bis(imino)pyridyl iron catalysts posses a linear structure. The linear structure of the samples was theoretically predicted in our group by computer simulations of the copolymerization of ethylene with 1-hexene [36], and it was also probed experimentally [28].

SEC results show a variation in the M_w of the samples. The data listed in Table 1 reveal that both M_w and M_w/M_n systematically increase as the presence of hydrogen during polymerization does from PE2 to PE4. Additionally, the materials are characterized by high values of M_z/M_w, indicating the presence of high-M_w tails. Huang and co-workers have argued that the presence of molecular hydrogen results in a greatly decreased formation of low M_w polymer in the case of catalysts with less hindered metal complexes [37]. Moreover, the reported data by these authors have suggested not only a decrease of the amount of low-M_w fraction but also an increase in the M_w and the amount of the high-M_w fraction of the MWD. These authors have concluded that the dominant effect of hydrogen in this less steric bulk system is the deactivation of active species that polymerize low M_w material and the activation of those species that produce the high M_w fraction. Recent computer simulations made in our group using global and local descriptors of chemical reactivity and selectivity based on the DFT theory, have shown that these catalysts produce materials with broad MWD and high-M_w species [25–27].

Concerning the physical properties, the materials with the lowest M_w values show increased density and crystallinity and decreased melting temperatures, similarly to analogous samples studied by other authors [37], and also to linear PE samples synthesized using single-site catalysts [38]. There are some differences among the samples studied here, but these are not expected to be due to the presence of short chain branches, as judged by the ^{13}C NMR results and the computer simulations. The apparent molecular weight dependence of the microstructural features is a well-know effect caused by the non-equilibrium conditions at which thermal properties are measured. The crystallization time during the DSC scan is similar in all the samples, but because of the different M_w, the time needed to reach equilibrium crystallization conditions is also different in each case. As the M_w increases, the chain movements are more restrained as a consequence of the increased average number of entanglements, and thus more time is required to reach the same state than the corresponding to a sample with a lower M_w value. This obviously gives rise to lower values of crystallinity and density in the samples with the highest M_w.

In addition to the considerations about the microstructure, the materials studied are of interest because of their rheological properties. The relationship between molecular features and rheological properties is a topic of long-standing discussion in polymer science, especially the dependence of η_0 and J_e^0 on the molecular features. We have measured the values η_0 of the materials under study from dynamic [29] and creep measurements. The creep measurements at 160 °C for the samples studied are shown in Fig. 1. In order to guarantee the linearity of the viscoelastic response in these experiments the results obtained at different shear stresses, τ_0, are compared (between 1.56 and 12.5 Pa). All the samples show linear behavior in the shear stress range explored. At long creep times all the samples show a straight line of a slope 1 in the double logarithmic plot, which is equal to a plateau in $t/J(t)$ versus t plot. This demonstrates that for the samples investigated the steady-state of creep is obtained and that the determination of η_0 is possible, by means of the application of Eq. (9). For the polydisperse PE samples the creep compliance decreases (viscosity increases) as the molecular mass increases, as expected. The results of η_0 obtained from these data are listed in Table 2, being in perfect agreement with those obtained previously from the dynamic measurements [29].

The $\eta_0 - M_w$ dependence is represented by the well-known relationship observed for many linear monodisperse polymers [39]:

$$\eta_0 = KM_w^{\alpha} \tag{11}$$

where, for PE, α takes values from 3.36 to 3.64 and K is a constant that depends on temperature [30]. This relationship is valid for M_w values above M_c, being M_c a critical molecular weight related to the molecular weight of an entanglement strand, M_e. Fig. 2A includes the results obtained for our polydisperse PE materials and other results obtained from the literature for polydisperse PE samples [3,7,10–12]. We have also included the reported correlation obtained for selected data of linear PE fractions, monodisperse hydrogenated polybutadiene and mPE samples with narrow MWD [30]. Significant deviations from the trend followed by monodisperse PE samples are observed for the polydisperse PE series studied in this work and for the most of the data collected from the literature. The presence of high-M_w tails could be the cause of this deviation, as it seems to be more pronounced as the value of M_z/M_w increases. For the materials with $M_z/M_w \sim M_w/M_n = 2–3$

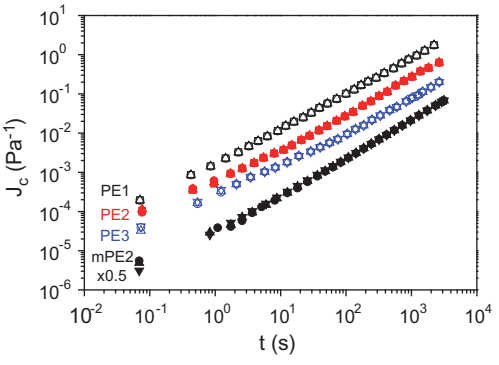

Fig. 1. Creep compliance versus creep time for the materials studied at $T = 160$ °C and different shear stresses: (squares) 1.56 Pa; (circles) 3.12 Pa; (up triangles) 6.25 Pa and (down triangles) 12.5 Pa. Creep compliance values for mPE2 sample have been shifted vertically (×0.5) to avoid crowding.

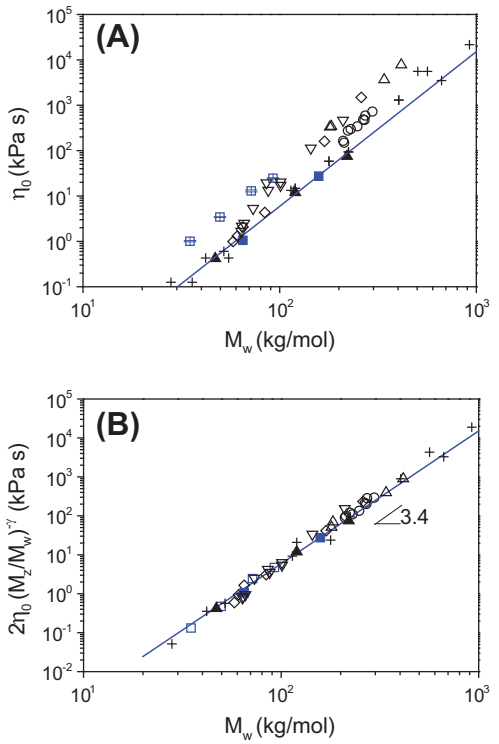

Fig. 2. (A) Newtonian viscosity versus weight average molecular weight at $T = 160$ °C (□) polydisperse PE samples, (■) mPE with narrow MWD, (▽) polydisperse HDPE with $M_z/M_w = 3.0–5.4$ [3], (◇) polydisperse HDPE with $M_z/M_w = 2–9$ [7]; (+) mHDPE with narrow MWD with $M_z/M_w = 2.2–3.5$ [10], (○) polydisperse mHDPE with $M_z/M_w = 3–5$ [11], (▲) HDPE with narrow MWD [12], (△) polydisperse HDPE with $M_z/M_w = 6.5–11.2$ [12]. The solid line corresponds to the correlation found for monodisperse HDPE fractions and mPEs [30]. (B) Weight-average molecular weight dependence of the normalized Newtonian viscosity for the materials studied at $T = 160$ °C. The symbols are the same than in Fig. 2A.

[10,12], including our mPE samples with narrow MWD (crosses and solid symbols in Fig. 2A), the deviation from the correlation of monodisperse samples is only marginal. This result suggests that in this type of materials (single-site catalyzed PE samples) the amount of high-M_w tails is not high enough to cause an impact in the values of η_0, with respect to that exhibited by linear monodisperse PE samples with the same M_w. In fact, the term $(M_z/M_w)^{0.8}$ cancels the pre-exponent 0.51 in Eq. (1) for values of M_z/M_w around 2.0 [29]. In contrast, the materials with values of $M_z/M_w = 4.0–11.2$ [3,7,11,12] clearly deviate from the correlation (open symbols in Fig. 2A), and also our polydisperse PE samples with the highest M_z/M_w ever measured in this type of polymers to our knowledge. These results suggest that polydispersity index given as M_w/M_n is not enough to judge the effect of the MWD on the linear viscoelastic behavior.

However, additional interpretations further than high-M_w tails, could lead us to argue on the possible presence of molecules with long chain branches (LCB) in the samples studied. In the last decade a significant number of studies have been carried out in order to establish the exact η_0–M_w relationship in PE. The reason behind that is its potential use as an indirect method to determine the amount of LCB in polyolefins and to differentiate its effect from that induced by the MWD. In particular, low LCB contents (less than 1 branch per 10,000 carbon atoms) lead to substantial increments in η_0 values in comparison with that exhibited by the linear counterpart in samples obtained from single-site catalysts [40–42]. These catalyst systems cannot only produce polyolefins with narrow MWD and LCB, but they also show the capacity to incorporate high amounts of comonomer. The most probable mechanism to produce LCB in this type of polymerization is terminal branching [43]. In this mechanism, terminated chains formed during the polymerization process by β-hydride elimination reaction or by transfer to ethylene are inserted in another growing chain, as occurs in a copolymerization step. These terminated chains containing vinyl-end groups act as macro-monomers. Thus to form a LCB, the copolymerization ability of the catalyst is a necessary condition. Notwithstanding, it has been reported both experimentally and theoretically the inefficiency of the catalyst used here for the incorporation of either α-olefin as 1-hexene [28,36], or even more bulky comonomers as styrene [44]. In addition to this, it should be noted that PE is one of the few polymers for which the presence of LCB affects the temperature dependence of rheological properties [45]. In fact, the values of E_a increases as LCB content does in PE samples with branching content between 0.1 and 1 branches per 10,000 carbon atoms [46]. For these samples the observed increase of η_0 of nearly one order of magnitude (same as the observed in the materials under study) with respect to the linear species, would corresponds to LCB contents close to 1 branch per 10,000 carbon atoms and values of E_a of close to 40 kJ mol^{-1} [42]. In our samples an average value of $E_a = 26.7 \pm 1.3$ kJ mol^{-1} has been obtained, which is consistent with the reported value of linear PE, so the presence of LCB should be completely ruled out.

Then the effect should definitively be due to the presence of very high-M_w tails in the MWD of the samples. Interestingly, the samples studied show a strong positive asymmetric deviation in the MWD with respect to the mean value, as it can be observed in Fig. 3. The positive deviation accounts for closely the 20% of the whole MWD within the molecular weight range from 10 to 10,000 kg mol^{-1}. This deviation of the MWD causes extremely high M_z/M_w ratio values of around 20–30, as it has been pointed out in preceding lines. Additionally, the values of M_z/M_w are higher than the polydispersity index, M_w/M_n, in all the cases (the maximum value of M_w/M_n in Table 1 is 13.3). The characteristic high M_z/M_w values in the samples are related to the existence of a large number of components with high relaxation times contributing to the linear viscoelastic response. In the framework of Eq. (1), using the pre-exponential factors given by Nobile and Cocchini [8] used also in our previous work [29], it is possible to fit all the data in Fig. 2A to a single correlation considering variable values of γ, depending of the sample series considered. The result of the fitting can be observed in Fig. 2B. Our polydisperse PE samples fit very well by considering a value of $\gamma = 0.80$ [29]. For the results taken from the literature (shifted to $T = 160$ °C by using the characteristic value of E_a for linear PE), the fitting requires values of

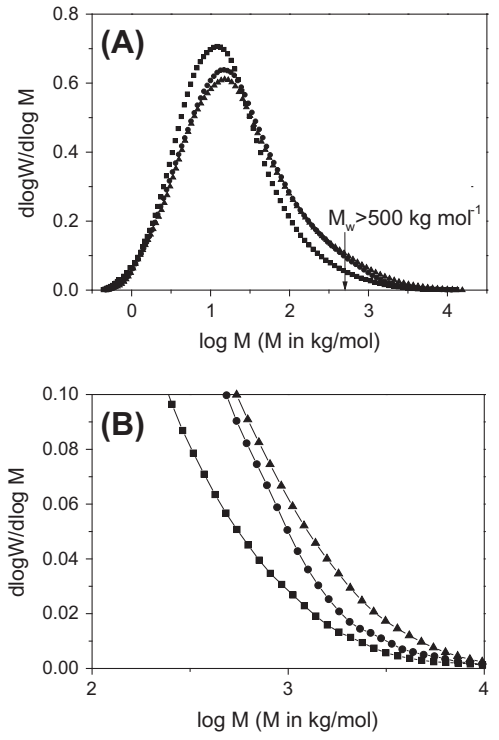

Fig. 3. SEC traces of some of the samples studied: (■) PE2; (●) PE 3 and (▲) PE4.

γ ranging from 1.0 [7,11] to 1.30 [8,10,12]. The average value obtained for γ for the whole set of materials is around 1.0, which is in agreement with the empirical correlations reported in the literature [5,7] and close to the theoretical values of 0.7–0.8 [8,9]. The variability found in the values of γ is higher than the experimental uncertainly expected in η_0 (±20–30%) due to the variability in the measurement of MWD by SEC (±5–10%). A proper determination of both η_0 and MWD is crucial, which is particularly problematic in the case of very high M_w polymers, i.e. above 300 kg mol^{-1} and broad MWD. Notwithstanding, it should be pointed out that the investigated extremely broad PE samples with M_z/M_w significantly larger than M_w/M_n are experimental specimens with little relevance to commercial products for which the independence of η_0 on the MWD is a very good approximation [10,30].

The presence of these very high-M_w components should have an important impact not only in η_0 values, but also in the elastic character of the materials. The values of J_e^0 are usually better determined in creep and creep-recovery experiments than in oscillatory shear tests. There are various reasons for the use of creep and creep-recovery tests in determining this viscoelastic function [47–51]: (i) the steady-state of deformation is reached much faster than in oscillatory shear [47]; (ii) oscillatory shear measurements are sometimes limited due to torque transducer accuracy in the low frequency range of the rheometers [48]. In this region for loss angles close to $\delta = 90°$ the resolution affects G' more than G''. This fact makes possible to achieve η_0 from G'', but conversely it makes extremely difficult to obtain J_e^0 from G'. For these reasons creep and creep recovery test is a more suitable technique for the determination of this viscoelastic function. Examples of the creep and creep-recovery tests performed to obtain J_e^0 are given in Fig. 4A–C for three of the samples studied: PE3, PE4 and mPE2. The applied stress values, $\tau_0 = 3.12$ and 12.5 Pa, respectively, are within the linear viscoelastic range as it is demonstrated in Fig. 1: identical time dependence of J_c are obtained in all the cases in this range of shear stress. However, it has been reported in the literature that the recoverable compliance also depends on the creep time, t_c [48]. In the case of the polydisperse PE samples studied the values of the J_r plateau at long times are highly dependent on t_c, as it can be observed in Fig. 4A for the PE3 sample. Constant values of J_e^0 are reached for t_c values of 1250 s and higher for an applied shear stress of $\tau_0 = 3.12$ Pa. An increase of more than twice in t_c does not significantly change the final value of J_e^0. In order to assure that J_e^0 has really been achieved for the polydisperse PE samples we have additionally performed creep-recovery measurements at different shear stresses within the range 0.78–3.12 Pa and during high enough creep times of $t_c = 3{,}125$ s. As an example these tests are shown in Fig. 4B for PE4 sample. In this figure it is clearly seen that both J_c and J_r coincide, being the standard deviation of the final value of J_e^0 measured of around s.d. = ±3.5%. Similar results about the linearity of the response were obtained for the other polydisperse PE products in the same range of shear stress and creep time. In the case of mPE2 sample a higher value of the shear stress ($\tau_0 = 12.5$ Pa) has been applied to achieve a higher resolution of the rheometer. In this case, and in contrast to polydisperse PE samples, the steady state value is reached after quite short recovery times (Fig. 4C), in agreement with previous results obtained in materials with narrow MWD [49–51]. Also the value of J_e^0 obtained in this sample is in agreement with that reported for this type of materials ($J_e^0 \sim 0.06$–0.07 mPa^{-1}).

The most interesting feature observed in the polydisperse PE samples is the very high J_e^0 values obtained, being between 200 and 1000 times higher than that obtained for the mPE2 sample. Moreover, the increase observed in J_e^0 values in the polydisperse series is not explained by the different M_w of the samples. In fact an apparent decrease of J_e^0 as M_w increases is directly read from the results in Table 2 for this series. The value of J_e^0 of a polymeric material depends on a number of molecular parameters. From the literature it is known that for linear monodisperse polymers above the critical molar mass J_e^0 is molar mass independent [52], but increases with the broadening of the MWD. As it has been pointed out in the introduction, different empirical and theoretical correlations between J_e^0 and the MWD can be found in the literature. Fig. 5A depicts the experimental values of J_e^0 for the materials studied in the present work together with experimental data collected from the literature for linear PE, including model hydrogenated polybutadienes (HPB), in which M_z/M_w is available [11,14,53–56]. In the case of monodisperse HPB samples we have considered that $M_w/M_n = M_z/M_w$. These data were obtained at different temperatures within the range 150–190 °C. This should not affect to the

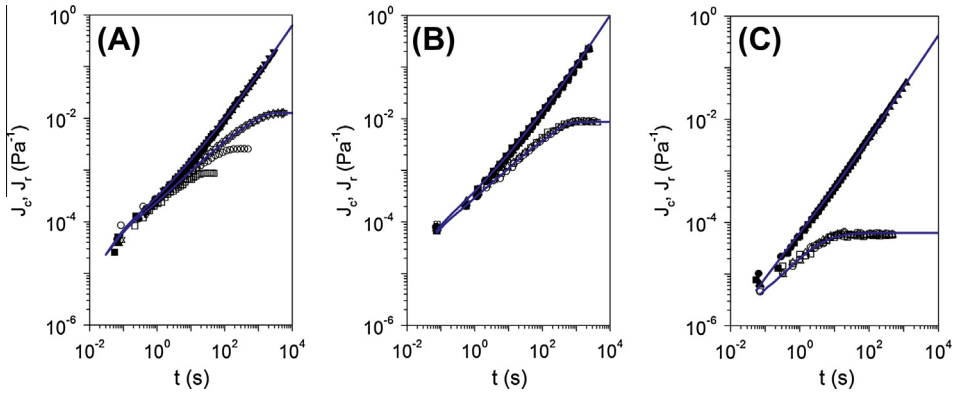

Fig. 4. Creep, J_c (solid symbols), and recovery compliance, J_r (open symbols), for the materials studied at $T = 160$ °C: (A) PE3 ($\tau_0 = 3.12$ Pa) and (C) mPE2 ($\tau_0 = 12.5$ Pa) with variable creep time, t_c (squares) 50 s, (circles) 250 s, (up triangles) 1250 s, (down triangles) 3125 s. (B) PE4 ($t_c = 3125$ s) with variable shear stress, τ_0 (squares) 0.78 Pa, (circles) 1.56 Pa and (triangles) 3.12 Pa.

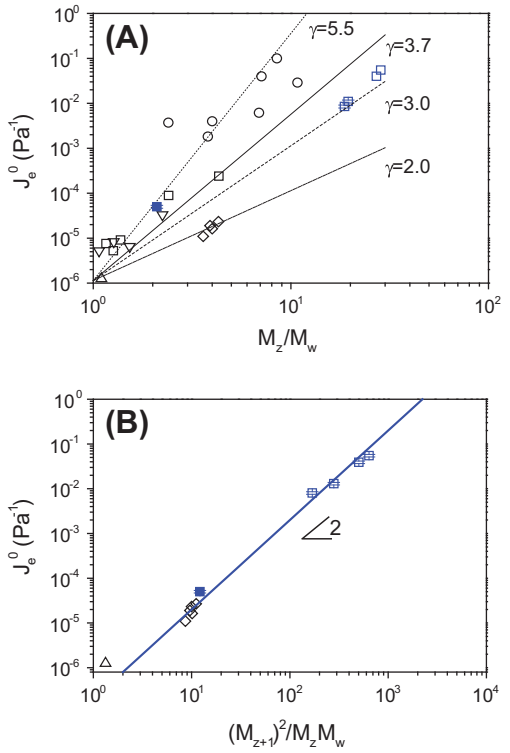

Fig. 5. (A) Steady-state shear recoverable compliance, J_e^0, versus M_z/M_w for the materials studied at $T = 160$ °C; (■) polydisperse PE samples and (■) mPE2, and literature results for linear polydisperse PE samples; (■) Mills et al. [53]; (○) Plazek et al. [54]; (△) HPB from Carella et al. [55]; (▽) Yoshikawa et al. [56] and (◇) Ansari et al. [11]. The lines correspond to Eq. (2) with different exponents: (solid line) $\gamma = 3.7$ [13], (dashed-dotted line) $\gamma = 2.0$ [15], (dashed line) $\gamma = 3.0$ [16], and (dotted line) $\gamma = 5.5$ [8]. (B) Correlation between J_e^0 and a measure of MWD, M_{z+1}^2/M_zM_w, for the materials under study and for materials from the literature. The symbols are the same than in Fig. 5A. The slope is 2.0 as it is expected according to Eq. (6) [9].

comparison, as J_e^0 is temperature independent in a thermorheologically simple polymer as linear PE [56]. Also Eq. (2) is plotted considering the different exponents proposed by Mieras and van Rijn ($\gamma = 3.7$), Bogue et al. ($\gamma = 2.0$), Kurata ($\gamma = 3.0$) and Nobile and Cocchini ($\gamma = 5.5$). An increase of the experimental values of J_e^0 with M_z/M_w is observed as a general trend. However, each correlation seems to explain the behavior of a particular series. It should be pointed out that, except the experimental results recently reported by Ansari et al. [11], which follow the squared power law reported by Bogue et al. [15], the other results seem to deviate towards the Kurata ($\gamma = 3.0$) and/or Nobile and Cocchini ($\gamma = 5.5$) correlations. It should be also noted that for the most of the samples from the literature, detailed information on the molecular structure is missing. It is known that the presence of small amounts of LCB causes a strong effect in J_e^0 [49,50,57]. Another source for the data scattering could be the presence of tiny amounts of high-M_w tails (<1 wt.% with $M_w > 1000$ kg mol^{-1}), which will be hardly detected [58–60]. As it is clear from Fig. 5B, it is the correlation given by den Doelder (Eq. (6)) that best explains the results obtained in our materials and those recently reported by Ansari et al. [11]. The functional dependence of J_e^0 is then described by the MWD in the form of M_{z+1}^2/M_wM_z with a power law exponent of 2, suggesting the strong effect of the very high-M_w tail in this viscoelastic function. The verification of this dependence asks for a wider experimental support in well characterized samples with broad MWD. Unfortunately, we have not found additional results in the literature than those of Ref. [11] reporting both J_e^0 and M_{z+1} in linear PE samples in order to further test this correlation.

It is of interest to additionally check the experimental results obtained in both the creep-recovery and dynamic modes. The values of the shear creep, J_c, and shear recovery, J_r, compliances can be converted to the dynamic moduli, G' and G'', following the procedure described by Kaschta and Schwarzl [61]. This methodology has been widely used to obtain the complete linear viscoelastic fingerprint of polyolefins in the terminal region [48–51]. The discrete retardation spectra $\{\tau_k, J_k\}$ of the materials under study have been obtained by fitting both the experimental values of J_c and J_r to the following equations [35]:

$$J_c(t) = J_0 + \sum_{K=1}^{n} J_k(1 - e^{-t/\tau_k}) + \frac{1}{\eta_0} \qquad (12)$$

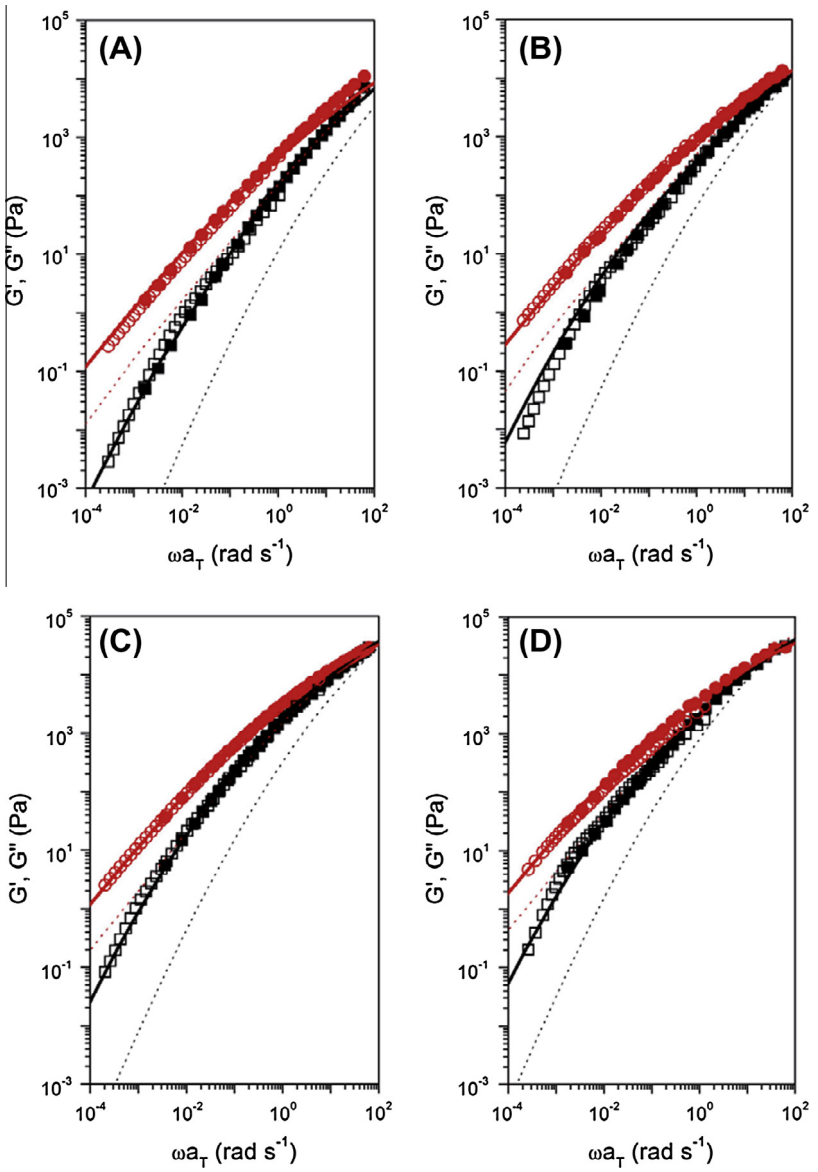

Fig. 6. Comparison of the experimental (symbols) and computed (lines) linear viscoelastic response at the $T = 160$ °C of the samples studied: (A) PE1, (B) PE2, (C) PE3 and (D) PE4: squares for G' and circles for G'' (open symbols for creep-recovery converted data and solid symbols for oscillatory measurements). Solid lines correspond to the computed response using the experimental MWD obtained by SEC by the application of Eqs. (18)–(21). Dashed lines correspond to the computed response using equivalent log-normal MWD (same M_w and $M_w/M_n = M_z/M_n$).

$$J_r(t) = J_0 + \sum_{K=1}^{n} J_k(1 - e^{-t/\tau_k}) \tag{13}$$

The instantaneous compliance, J_0, has been considered negligible. The different sets of $\{\tau_k, J_k\}$ data have been found by using the Reptate software [62]. As examples, the solid lines in Fig. 4A–C are the results obtained for the fitting procedure applied to PE3, PE4 and mPE2 samples. Knowing the retardation spectra, the theory of linear viscoelasticity allows the conversion of the time-dependent compliances into the dynamic moduli as a function of the angular frequency, ω:

$$J'(\omega) = \sum_{K=1}^{n} J_k \frac{1}{1 + \omega^2 \tau_k^2} \tag{14}$$

$$J''(\omega) = \frac{1}{\omega \eta_0} + \sum_{K=1}^{n} J_k \frac{\omega \tau_k^2}{1 + \omega^2 \tau_k^2} \tag{15}$$

Finally, from the relation between the complex compliance $J^*(\omega)$ and the complex modulus $G^*(\omega)$, the following equations can be derived to extract the corresponding values of the storage and loss moduli, $G'(\omega)$ and $G''(\omega)$ as:

$$G'(\omega) = \frac{J'(\omega)}{[|J^*(\omega)|]^2} \tag{16}$$

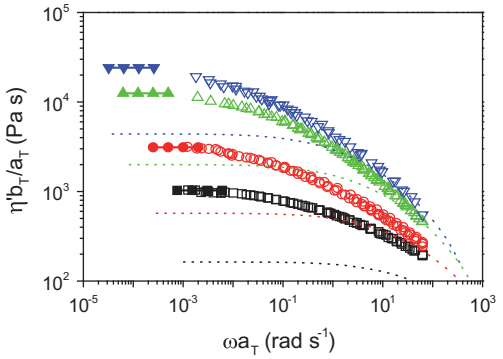

Fig. 7. Comparison of the experimental values (symbols) of the dynamic viscosity, η', versus angular frequency, ω, for the materials studied at $T = 160$ °C with those expected by the model for symmetrical log-normal MWD with the same M_w and M_w/M_n than the polydisperse PE samples studied (dotted lines): (□■) PE1, (○●) PE2, (△▲) PE3, (▽▼) PE4. The open symbols correspond to experimental dynamic measurements and the solid symbols to creep measurements.

$$G''(\omega) = \frac{J''(\omega)}{[|J^*(\omega)|]^2} \tag{17}$$

The calculation of the dynamic moduli has been restricted to the experimental window of the creep-recovery measurement. The calculated values have been compared with the experimental dynamic shear moduli that were directly measured at the same temperature. The dynamic shear moduli from calculations and measurements show a good agreement, as it can be seen in Fig. 6A–D. Additionally, the range for the dynamic shear moduli has been extended to lower frequencies, usually difficult to access in the oscillatory mode, as it has been pointed out in preceding lines.

It is also of interest to apply the general double reptation mixing rule to obtain the whole linear viscoelastic response of the materials in the broad range of frequencies explored (close to six decades) by making use of the experimental MWD obtained by SEC. Within the double reptation theory framework the expression for the relaxation modulus, $G(t)$, reads:

$$G(t) = G_N^0 \left[\int_{\log M_e}^{\infty} F^{1/2}(t, M) w(M) d\log M \right]^2 \tag{18}$$

In this equation $F(t, M)$ is the kernel function describing the relaxation of a molecular weight fraction, $w(M)$, G_N^0 is the plateau modulus and M_e the entanglement molecular weight. The exponent in this mixing rule was derived theoretically; the Doi-Edwards' reptation model yielded the linear mixing rule with an exponent of 1 [63], and the quadratic mixing rule was obtained by des Cloiseaux and Tsenoglou for double reptation [64,65]. Other approaches as dynamic dilution or the Rouse-like motion of the tube considered a slightly higher value of 7/3 [66–68]. Considering the double reptation approach, the kernel function in Eq. (18) can be obtained from the tube survival probability $\mu(t, M)$ of a chain with molecular weight M at time t established by the reptation theory [63,67]:

$$F^{1/2}(t, M) = \mu(t, M) = \frac{8G}{\pi^2} \sum_{p=odd}^{\infty} \frac{e^{-tp^2/\tau_d}}{p^2} \tag{19}$$

where G is the renormalization contour length fluctuations (CLF) factor for the modulus [66]:

$$G = 1 - \kappa \left(\frac{M_e}{M} \right)^{0.5} \tag{20}$$

and τ_d is the terminal relaxation time of a chain of molar mass M that includes the CLF effect on the basis of the entanglement relaxation time, τ_e [66,67]:

$$\tau_d = 3\tau_e \left(\frac{M}{M_e} \right)^3 \left[1 - \kappa \left(\frac{M_e}{M} \right)^{0.5} \right]^2 \tag{21}$$

being κ is a constant of the order unity. We have used in our calculations the value of $\kappa = 1.69$ obtained by Likhtman and McLeish [67]. The expression for τ_d provides the explanation for the decrease in the relaxation time as the molecular weight decreases, deviating from the predicted exponent 3.0 that holds for very long chains to the well-known value of 3.4 for shorter chains [60,69]. The other parameters of the model are the entanglement features: the plateau modulus, G_N^0, the molecular weight between entanglement strands, M_e, and the entanglement strand relaxation time, τ_e. We have recently obtained all these parameters for linear PE, by combining experiments and melt atomistic computer simulations [70,71]. These values are: $G_N^0 = 2.17 \pm 0.23$ MPa (experimental average), $M_e = 0.790 \pm 0.010$ kg mol^{-1} (Monte Carlo and Molecular Dynamics computer simulation) and $\tau_e = 2.50 \pm 0.12$ ns (Molecular Dynamics computer simulation) at $T = 160$ °C. This later value has been calculated from the obtained by computer simulations at $T = 177$ °C, by applying the corresponding temperature shift factor of linear PE. The calculated values of G' and G'' are found by appropriate Fourier transform of the results obtained for $G(t)$ from Eqs. (18)–(21).

Fig. 6A–D shows the comparison between the calculated and the experimental results in the polydisperse PE samples listed in Table 1. The agreement between the model and the experimental data is exceptional, taking into account the complex shape of the MWD and the differences among the samples. Additionally, it should be mentioned that no empirical or fitting parameters have been used to calculate the values of dynamic moduli. We have compared in the same figures the experimental results with those obtained from the model with the consideration of ideal Gaussian MWD functions with the same M_w and M_w/M_n than those obtained by SEC in the samples. The model has been widely reported to describe the linear viscoelastic fingerprint in linear polymers with very different shape in the MWD, including generalized exponential functions (GEX) [8], Gaussian or log-normal distributions [69,70] and multimodal log-normal combinations [9,60]. As it can be observed in Fig. 6, the predicted rheological response of a log-normal distribution is shifted to higher frequencies, pointing towards to a minor contribution of high-M_w species in the linear viscoelastic fingerprint. This shift to higher frequencies causes a difference in the

viscosity, which is one order of magnitude lower than the measured for the polydisperse PE samples with the same M_w and M_w/M_n (but different M_z/M_w) as it can be appreciated in Fig. 7. The results in Figs. 6 and 7 suggest then a strong dependence of the linear viscoelastic response not only due to M_w/M_n, but also to the shape of the MWD. In fact, as it has been pointed out in the introduction, this dependence has been widely discussed in the literature, but in the case of linear PE only for samples with values of the M_z/M_n ratio in the range 1.5–11.2 always lower or similar to M_w/M_n [7–18,53–56]. It should be then pointed out that the effects observed in the linear viscoelastic properties of the polydisperse PE samples studied here are not merely due to a broadening of the MWD in terms of M_w/M_n, but more precisely to the presence of a significant fraction of very high-M_w species, as judged by the extremely high values of M_z/M_w (2–5 times higher than M_w/M_n) and to the contribution of the fourth moment of the distribution, M_{z+1}. These high values of M_z and M_{z+1} together with the asymmetric character of the MWD represent a good opportunity to test the influence of the high-M_w tail of the distribution in the physical properties of these linear polymers. The high-M_w tail of the distribution in linear PE, even for contents lower than 1% in weight, has a significant effect not only on the linear viscoelastic fingerprint but also on the non-linear behavior, and more precisely in the processing and extrudate instabilities regimes during extrusion processes, as we have also probed in previous works [58–60].

4. Conclusions

We have studied a series of experimental polyethylene samples with broad molecular weight distributions and a significant fraction of high molecular weight species. The analysis of the linear viscoelastic response of the materials shows a conspicuous increase of both the Newtonian viscosity and the steady-state shear recoverable compliance when compared with model linear samples with the same weight average molecular weight but narrower molecular weight distribution. In addition, the polymers exhibit the characteristic temperature dependence of viscoelastic properties of linear polyethylene, and previous experiments and computer simulations also showed the inefficiency of the catalyst used in the polymerization to incorporate other species than ethylene, such as vinyl macromonomers, to the growing polymer chains during the polymerization. In this context, the presence of long chain branching causing the variations observed should be ruled out. In fact, the reptation mixing rule, together with the Doi's relaxation kernel applied to linear chains dynamics, is able to predict the dynamic shear moduli using the experimental Size Exclusion Chromatography traces of the samples. This result confirms previous predictions about the contribution of the high molecular tail of the distribution to the melt linear viscoelastic response, which in the materials studied here seems to be very important, due to their extremely high values of the M_z/M_w ratio. It is of particular interest to recall that not merely the width of the molecular weight distribution is significant, but more precisely the shape and predominantly the third and the fourth moments of the distribution, M_z and M_{z+1}, which seem to play a key role in the viscous and elastic properties of the melt.

Acknowledgements

Thanks are due to the CICYT (MAT2009-12364 and MAT2012-36341) for financial support. J.R. acknowledges financial support through the Ramon y Cajal program: Contract RYC-2011-09585. The supply of the samples is acknowledged to Carlos Martín (Centro Tecnológico Repsol-YPF, Spain).

References

[1] Bueche F. Melt viscosity of polymers: effect of polydispersity. J Polym Sci 1960;43:527–30.
[2] Graessley WW. Viscosity of entangling polydisperse polymers. J Chem Phys 1967;47:1942–53.
[3] Saeda S, Yotsuyan J, Yamaguchi K. The relation between melt flow properties and molecular weight of polyethylene. J Appl Polym Sci 1971;15:277–92.
[4] Locati G, Gargani L. Dependence of zero-shear viscosity on molecular-weight distribution. J Polym Sci – Polym Lett Ed 1973;11:95–101.
[5] Malkin AY, Blinova NK, Vinogradov GV, Zabugina MP, Sabsai OY, Shalganova VC, et al. On the rheological properties of polydisperse polymers. Eur Polym J 1974;10:445–51.
[6] Zeichner GR, Patel PD. A comprehensive evaluation of polypropylene melt rheology. In: Second World Conference Chemical Engineering, Montreal, Canada 1981;6:333–7.
[7] Wasserman SH, Graessley WW. Prediction of linear viscoelastic response for entangled polyolefin melts from molecular weight distribution. Polym Eng Sci 1996;36:852–61.
[8] Nobile MR, Cocchini F. Predictions of linear viscoelastic properties for polydisperse entangled polymers. Rheol Acta 2000;39:152–62.
[9] den Doelder J. Viscosity and compliance from molar mass distributions using double reptation models. Rheol Acta 2006;46:195–210.
[10] Stadler FJ, Piel C, Kaschta J, Rulhoff S, Kaminsky W, Münstedt H. Dependence of the zero shear-rate viscosity and the viscosity function of linear high-density polyethylenes on the mass-average molar mass and polydispersity. Rheol Acta 2006;45:755–64.
[11] Ansari M, Hatzikiriakos SG, Sukhadia AM, Rohlfing DC. Rheology of Ziegler–Natta and metallocene high-density polyethylenes: broad molecular weight distribution effects. Rheol Acta 2011;50:17–27.
[12] Vittorias I, Lilge D, Baroso V, ·Wilhelm M. Linear and non-linear rheology of linear polydisperse polyethylene. Rheol Acta 2011;50:691–700.
[13] Mieras HJMA, van Rijn CFH. Elastic behaviour of some polymer melts. Nature 1968;218:865–6.
[14] Mills NJ. Elasticity of polydimethylsiloxane melts. Nature 1968;219:1249–50.
[15] Bogue DC, Masuda T, Einaga Y, Onogi S. A constitutive model for molecular weight and concentration effects in polymer blends. Polym J 1970;5:563–72.
[16] Kurata M, Osaki K, Einaga Y, Sugie T. Effect of molecular weight distribution on viscoelastic properties of polymers. J Polym Sci 1974;12:849–69.
[17] Ferry JD, Williams ML, Stern DJ. Slow relaxation mechanisms in concentrated polymer solutions. J Phys Chem 1954;58:987–92.
[18] Agarwal PK. A relationship between steady state shear compliance and molecular weight distribution. Macromolecules 1979;12:342–4.
[19] Ressia JA, Villar MA, Vallés EM. Influence of polydispersity on the viscoelastic properties of linear polydimethylsiloxanes and their binary blends. Polymer 2000;41:6885–94.
[20] Montfort JP, Marin G, Arman J, Monge Ph. Blending law for binary blends of fractions of linear polystyrene. Polymer 1978;19:277–84.
[21] Zang YH, Muller R, Froelich D. Influence of molecular weight distribution on viscoelastic constants of polymer melts in the terminal zone. New blending law and comparison with experimental data. Polymer 1987;28:1577–82.

[22] Small BL, Brookhart M, Bennett AMA. Highly active iron and cobalt catalysts for the polymerization of ethylene. J Am Chem Soc 1998;120:4049–50.
[23] Britovsek GJP, Gibson VC, Kimberley BS, Maddox PJ, McTavish SJ, Solan GA, et al. Novel olefin polymerization catalysts based on iron and cobalt. Chem Commun 1998;7:849–50.
[24] Mikenas TB, Zakharov VA, Echevskaya LG, Matsko MA. Kinetic features of ethylene polymerization over supported catalysts [2,6-Bis(imino)pyridyl iron dichloride/magnesium dichloride] with AlR_3 as an activator. J Polym Sci Part A – Polym Chem 2007;45:5057–66.
[25] Cruz VL, Ramos J, Gutiérrez-Oliva S, Toro-Labbé A, Martínez-Salazar J. Theoretical study on a multicenter model based on different metal oxidation states for the bis(imino)pyridine iron catalysts in ethylene polymerization. Organometallics 2009;28:5889–95.
[26] Cruz VL, Martínez J, Martínez-Salazar J, Ramos J, Reyes ML, Toro-Labbé A, et al. QSAR model for ethylene polymerisation catalysed by supported bis(imino)pyridine iron complexes. Polymer 2007;48:7672–8.
[27] Martínez J, Cruz V, Ramos J, Gutiérrez-Oliva S, Martínez-Salazar J, Toro-Labbé A. On the nature of the active site in bis(imino)pyridyl iron, a catalyst for olefin polymerization. J Phys Chem C 2008;112:5023–8.
[28] Vega JF, Otegui J, Exposito MT, Lopez M, Martín C, Martínez-Salazar J. Structure and physical properties of polyethylenes obtained from dual catalysis process. Polym Bull 2008;60:331–42.
[29] Vega JF, Otegui J, Ramos J, Martínez-Salazar J. Effect of molecular weight distribution on Newtonian viscosity of linear polyethylene. Rheol Acta 2012;51:81–7.
[30] Aguilar M, Vega JF, Sanz E, Martínez-Salazar J. New aspects on the rheological behavior of metallocene catalysed polyethylenes. Polymer 2001;42:9713–21.
[31] Grubisic Z, Rempp P, Benoit H. A universal calibration for gel permeation chromatography. J Polym Sci Part B – Polym Lett 1967;5:753–9.
[32] Drott EE, Mendelson RA. Determination of polymer branching with gel-permeation chromatography. II. Experimental results for polyethylene. J Polym Sci Part A2 Polym Phys 1970;8:1373–85.
[33] Cote JA, Shida M. Long-chain branching in low-density polyethylene. J Polym Sci Part A2 – Polym Phys 1971;9:421–30.
[34] Williamson GR, Cervenka A. Characterization of low-density polyethylene by gel permeation chromatography-I. The universal calibration curve and Mark-Houwink equation. Eur Polym J 1972;8:1009–17.
[35] Ferry JD. Viscoelastic properties of polymers. 3rd ed. New York: Jon Wiley and Sons; 1980.
[36] Ramos J, Cruz V, Muñoz-Escalona A, Martínez-Salazar J. A computational study of iron-based Gibson–Brookhart catalysts for the copolymerisation of ethylene and 1-hexene. Polymer 2002;43:3635–45.
[37] Huang R, Koning CE, Chadwick JC. Effects of hydrogen in ethylene polymerization and oligomerization with magnesium chloride-supported bis(imino)pyridyl iron catalysts. J Polym Sci Part A – Polym Chem 2007;45:4054–61.
[38] Piel C, Stadler FJ, Kaschta J, Rulhoff S, Münstedt H, Kaminsky W. Structure-property relationships of linear and long-chain branched metallocene high-density polyethylenes characterized by shear rheology and SEC-MALLS. Macromol Chem Phys 2006;207:26–38.
[39] Berry GC, Fox TG. The viscosity of polymers and their concentrated solutions. Adv Polym Sci 1967;5:261–357.
[40] Vega JF, Santamaría A, Muñoz-Escalona A, Lafuente P. Small-amplitude oscillatory shear flow measurements as a tool to detect very low amounts of long chain branching in polyethylenes. Macromolecules 1998;31:3639–47.
[41] Malmberg A, Liimatta J, Lehtinen A, Lofgren B. Characteristics of long chain branching in ethene polymerization with single site catalysts. Macromolecules 1999;32:6687–96.
[42] Wood-Adams PM, Dealy JM, DeGroot AW, Redwine OD. Effect of molecular structure on the linear viscoelastic behavior of polyethylene. Macromolecules 2000;33:7489–99.
[43] Soares JBP, Hamielec AE. Bivariate chain length and long chain branching distribution for copolymerization of olefins and polyolefin chains containing terminal double-bonds. Macromol Theor Simul 1996;5:547–72.
[44] Expósito MT. Ph.D. Thesis. Universidad Complutense de Madrid, Madrid (Spain); 2006.
[45] Carella JM, Gotro JT, Graessley WW. Thermorheological effects of long-chain branching in entangled polymer melts. Macromolecules 1986;19:659–67.
[46] Wood-Adams P, Costeux S. Thermorheological behavior of polyethylene: effects of microstructure and long chain branching. Macromolecules 2001;34:6281–90.
[47] Gabriel C, Kaschta J. Comparison of different shear rheometers with regard to creep and creep recovery measurements. Rheol Acta 1998;37:358–64.
[48] Gabriel C, Kaschta K, Münstedt H. Influence of molecular structure on rheological properties of polyethylenes. I. Creep recovery measurements in shear. Rheol Acta 1998;37:7–20.
[49] Gabriel C, Münstedt H. Creep recovery behavior of metallocene linear low-density polyethylenes. Rheol Acta 1999;38:393–403.
[50] Gabriel C, Münstedt H. Influence of long-chain branches in polyethylenes on linear viscoelastic flow properties in shear. Rheol Acta 2002;41:232–44.
[51] Stadler F, Münstedt H. Terminal viscous and elastic properties of linear ethane/α-olefin copolymers. J Rheol 2008;52:697–712.
[52] Dealy JM, Larson RG. Structure and rheology of molten polymers. Munich: Hanser Publishers; 2006.
[53] Mills NJ. The rheological properties and molecular weight distribution of polydimethylsiloxane. Eur Polym J 1969;5:675–95.
[54] Plazek DJ, Ragupathi N, Kratz RF, Miller WR. Recoverable compliance behavior of high-density polyethylenes. J Appl Polym Sci 1979;24:1305–20.
[55] Carella JM, Graessley WW, Fetters LJ. Effects of chain microstructure on the viscoelastic properties of linear polymer melts: polybutadienes and hydrogenated polybutadienes. Macromolecules 1984;17:2775–86.
[56] Yoshikawa K, Toneaki N, Moteki Y, Takahashi M, Masuda T. Dynamic viscoelastic, stress relaxation and elongational flow behavior of high density polyethylene melts. In: Collier I, Utracki LA, editors. Polymer rheology and processing. New York: Elsevier; 1990. p. 37–53.
[57] Resch JA, Stadler FJ, Kaschta J, Munstedt H. Temperature dependence of the linear steady-state shear compliance of linear and long-chain branched polyethylenes. Macromolecules 2009;42:5676–83.
[58] Aguilar M, Expósito MT, Vega JF, Muñoz-Escalona A, Martínez-Salazar J. Elimination of extrudate distortions in metallocene-catalyzed polyethylene. Macromolecules 2004;37:681–3.
[59] Aguilar M, Martín S, Vega JF, Muñoz-Escalona A, Martínez-Salazar J. Processability of a metallocene-catalyzed linear PE improved by blending with a small amount of UHMWPE. J Polym Sci Part B – Polym Phys 2005;43:2963–71.
[60] Vega JF, Expósito MT, Otegui J, Martínez-Salazar J. Eliminating sharkskin distortion in polyethylene extrusion via a molecular route. J Rheol 2011;55:855–74.
[61] Kaschta J, Schwarzl ER. Calculation of discrete retardation spectra from creep data-I. Method Rheol Acta 1994;33:517–29.
[62] Ramírez J, Likhtman A. Rheology of Entangled Polymers: Toolkit for Analysis of Theory and Experiment. <http://www.reptate.com>.
[63] Doi M, Edwards SF. The theory of polymer dynamics. Oxford: Clarendon; 1986.
[64] Tsenoglou C. Viscoelasticity of binary homopolymer blends. Am Chem Soc Polym Prep – Div Polym Chem 1987;28:187–8.
[65] des Cloizeaux J. Double reptation vs simple reptation in polymer melts. Europhys Lett 1988;5:437–42.
[66] Milner ST, McLeish TCB. Parameter-free theory for stress relaxation in star polymer melts. Macromolecules 1997;30:2159–66.
[67] Likhtman AE, McLeish TCB. Quantitative theory for linear dynamics of linear entangled polymers. Macromolecules 2002;35:6332–43.
[68] van Ruymbeke E, Keunings R, Stephenne V, Hagenaars A, Bailly C. Evaluation of reptation models for predicting the linear viscoelastic properties of entangled linear polymers. Macromolecules 2002;35:2689–99.
[69] Vega JF, Rastogi S, Peters GWM, Meijer HEH. Rheology and reputation of linear polymers. Ultra high molecular weight chain dynamics in the melt. J Rheol 2004;48:63–678.
[70] Ramos J, Vega JF, Theodorou DN, Martínez-Salazar J. Entanglement relaxation time in polyethylene: simulation versus experimental data. Macromolecules 2008;41:2959–62.
[71] Ramos J, Vega JF, Martínez-Salazar J. Assessment of entanglement features and dynamics from atomistic simulations and experiments in linear and short chain branched polyolefins. Soft Matter 2012;8:6256–63.